Stiffener configurations of beam to concrete-filled tube column connections

Abdelrahim K. Dessouki [a], Ahmed H. Yousef [*] and Mona M. Fawzy [b]

Structural Engineering Department, Faculty of Engineering, Ain Shams University, Egypt

Abstract.   The objective of this research is to study the ultimate moment capacity of the connections between steel I-beams and concrete-filled steel tube columns using different stiffener configurations. The main parameters considered are column cross section shape, square or circular, and filling the column with concrete. This analytical study includes finite element models using ANSYS program taking geometric and material nonlinearities into consideration. These models are verified against the experimental results obtained from previous researches and current design guides. The results show that using proper stiffener configuration affects the stress distribution through the connection and increases the ultimate moment capacity of the connections. Also, circular column is advantageous than the square column for all stiffener configurations and dimensions.

1. Introduction

Recently, concrete-filled steel tube (CFT) has drawn a widespread interest as column members of steel structures. Compared to conventional steel or other composite columns, these columns possess many advantages such as confinement and convenient formwork for the concrete core provided by the steel tube. Also, it improves stability and stiffness of the steel tube owing to the concrete filled into the column, and lower construction cost. While many advantages exist, their use in building construction has been limited due to the lack of construction experience and the complexity of connection detailing. These components have yet to be investigated to bring about their full potential with respect to their applications.

Several upgrading strategies can be applied in the connection, such as using different column cross section shapes with various stiffener configurations. Regarding the connections of CFT, the most convenient connection is to attach the steel I-beam through an external stiffener. This is an efficient method concerning both manufacturing and casting concrete inside the column. The stiffener reduces the stress concentration at the column steel wall preventing it from failure.

---

*Corresponding author, Associate Professor, E-mail: a_h_yousef69@yahoo.com
[a] Professor of Steel Structures and Bridges
[b] Ph.D. Student

Therefore, recent investigations have focused on the development of various shapes of stiffeners. Numerous research works have recently been carried out studying the variation of ultimate moment capacity of the connections between steel I-beams and CFT columns. The static strength of steel I-beam to rectangular hollow column section connections was investigated both experimentally and numerically (Lu 1997). Lu also studied the influence of concrete filling of the columns as well as the effect of composite and steel floors on the behavior and strength of such connections. The performance of CFT column-to-H beam connections with vertical stiffener plates was investigated by Kimura *et al*. (2005). Besides, the connection details and shear strength in the panel zone of CFT through beam connections were studied by Azizinamini (2005). Kim *et al*. (2008) studied the stress-transfer mechanism of CFT column-to-beam connections with external T-stiffener using experimental and numerical programs. The influence of local geometric details such as a horizontal element, a vertical element, and a hole in the horizontal element was investigated. Nonlinear finite element models of the two kinds of joints, namely steel bars headed through the pipe joint and steel bars welded with the upper strengthened ring joint, under the cyclic loading are established by Wang *et al*. (2010). It was demonstrated that if the material constitutive relation, calculation model and failure criterion is selected suitably, the FEM can accurately predict the overall seismic behavior and the inelastic performance of these two kinds of joints. This research investigates four different external stiffener configurations for I-beam to CFT column connections, as shown in Fig. 1. The stiffener shape (1) is the familiar one which was used previously by many researchers followed by stiffener shape (3); however, the other two stiffener shapes were rarely addressed despite their constructability advantages.

The purpose of this study is to demonstrate the effect of stiffener configurations on the ultimate moment capacity of the connections between steel I-beams and concrete-filled steel tube columns. A parametric study is carried out taking into consideration stiffener dimensions, column cross section as well as filling the column with concrete. Moreover, the effect of column cross section shape is considered by comparing the ultimate moment of the connections using square column
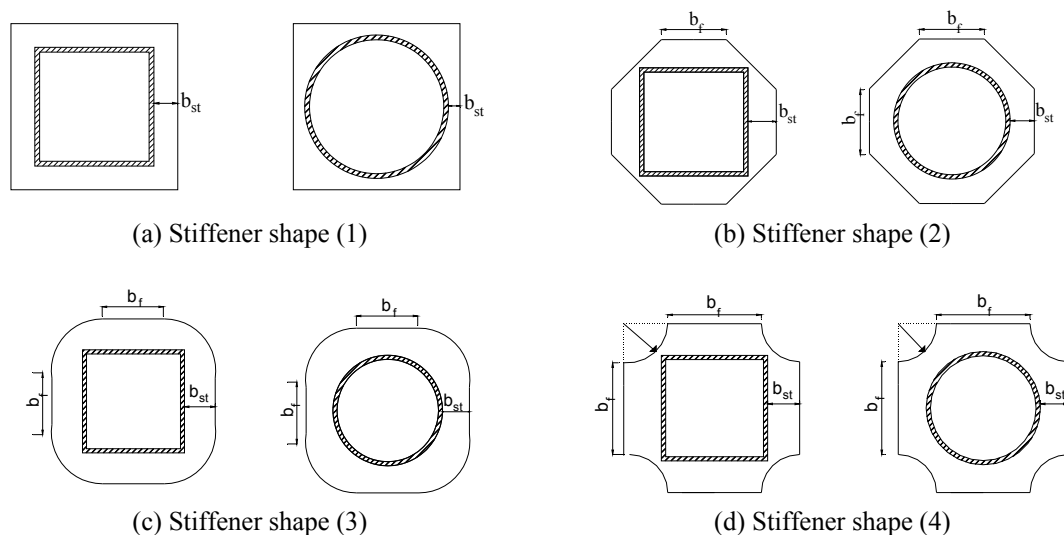

(a) Stiffener shape (1) (b) Stiffener shape (2)

(c) Stiffener shape (3) (d) Stiffener shape (4)

Fig. 1 Different stiffener shapes used in the research

with an equivalent area of steel and concrete-filling to circular column. The analyticalinvestigation utilizes nonlinear finite element modeling techniques using ANSYS program (2009). Finally, the finite element results are compared to one of the available current design guides (Kurobane *et al.* 2004).

2. Stiffener configurations

The stiffener attempts to transfer the forces through the connection, but stress concentrations are formed at corners, which become possible locations of failure by local buckling. Gradual transition of geometry is important in ensuring smooth flow of forces, which necessitates the development of various stiffener configurations. Stiffener shape (3) provides better force flow path towards the beam flanges followed by stiffener shapes (2) and (1), while stiffener shape (4) is the weakest. The comparison between results using different stiffener configurations will be discussed later in Section 6.

3. Finite element analysis

The finite element method is used to study the structural behavior of moment connections of steel I-beams and CFT columns incorporating all material properties and dimensions. The structural elements are divided into a number of finite elements with an aspect ratio of about one, as shown in Fig. 2. The finite element model details are described in the following subsections.

3.1 Modelling of steel parts, concrete, and steel to concrete contact

Four-node quadrilateral shell element SHELL43 is used to model the steel parts. It has membrane and bending capabilities and has six degrees of freedom at each node: three translations and three rotations. At both ends, the columns are connected to rigid end plates to distribute the load and reduce stress concentration. SOLID65 element is used to simulate concrete. It can simulate tension cracking, crushing, plastic deformation and creep of concrete in three orthogonal directions. The contact between the steel tube and the concrete is modelled by CONTA174 interface elements (Ju et al. 2004). Those interface elements consist of two matching contact faces of steel tube and concrete elements. The friction between the two faces is maintained as long as they remain in contact. The interface elements allow the surfaces to separate under the influence of tensile force. However, contact elements are not allowed to penetrate each other.

3.2 Material properties

Material properties of steel parts are defined by bilinear stress strain curve as shown in Fig. 3. Initial elastic modulus of elasticity is 200 kN/mm^2 and the strain hardening modulus of elasticity is defined as 0.01 of the initial elastic modulus. Steel grade 52 is used with specified yield stress equal to 360 N/mm^2. Poisson's ratio is assumed to be 0.3. A uniaxial compressive stress strain relationship, shown in Fig. 4, is used to model concrete in compression (Gere and Timoshenko 1997). The shear transfer coefficient which represents conditions of the crack face ranges from 0.0 smooth crack to 1.0 rough crack. The coefficient for the open crack was set to 0.2 while the coefficient for the closed crack was set to 1.0. Behavior of concrete in tension is assumed to be
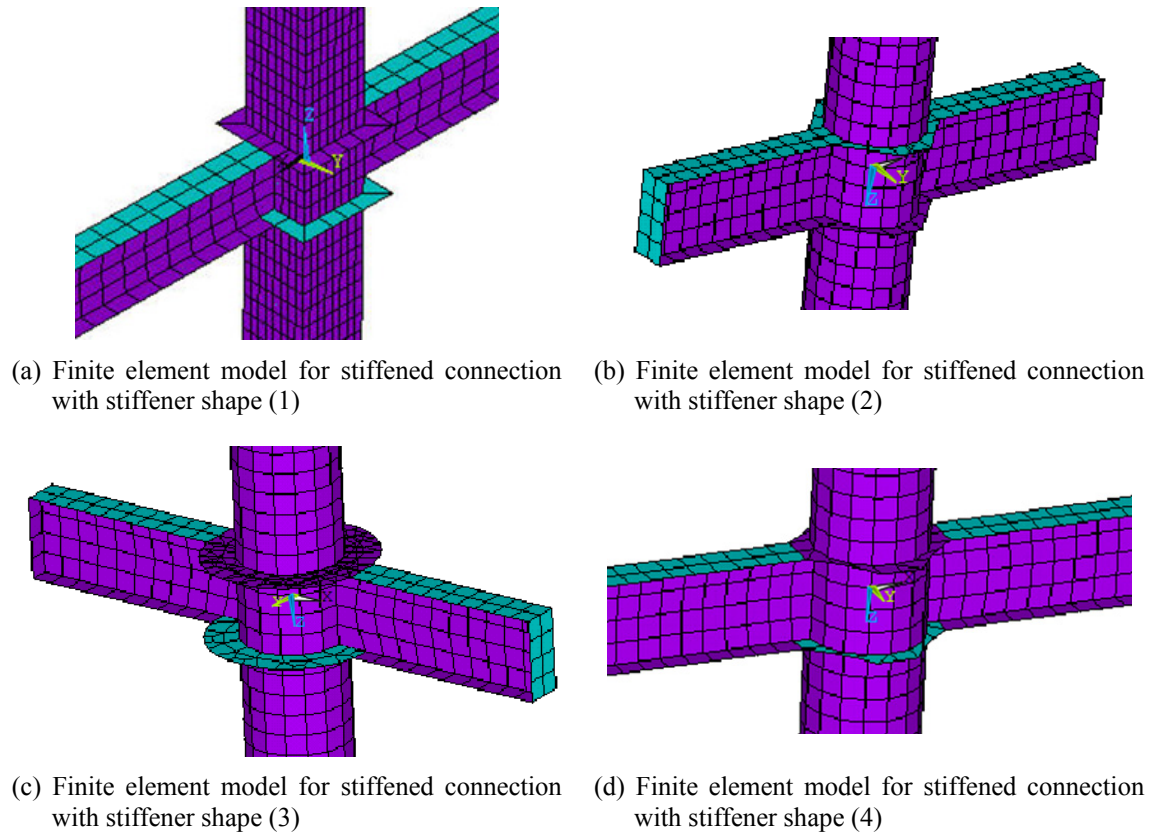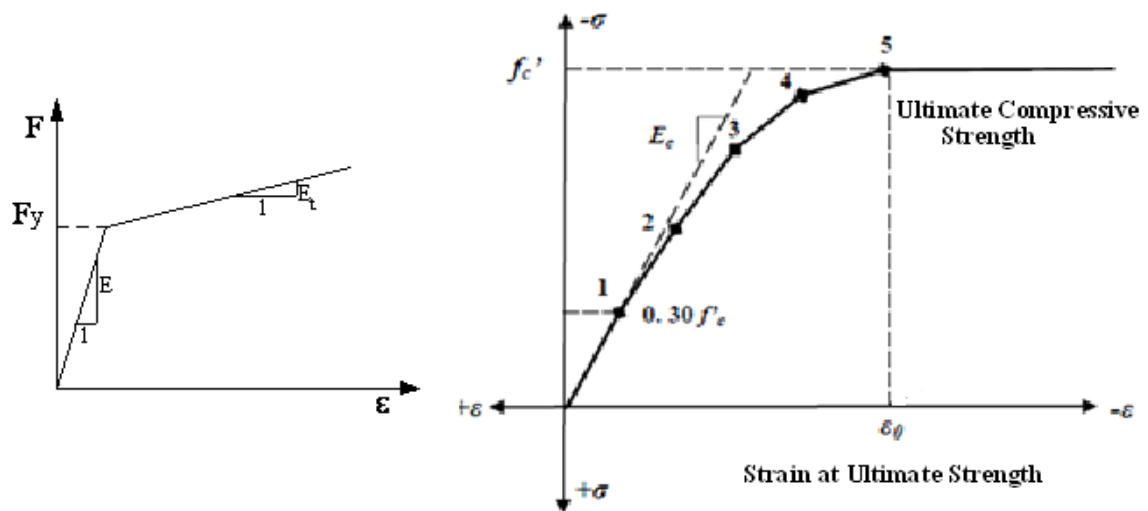
(a) Finite element model for stiffened connection
    with stiffener shape (1)

(b) Finite element model for stiffened connection
    with stiffener shape (2)

(c) Finite element model for stiffened connection
    with stiffener shape (3)

(d) Finite element model for stiffened connection
    with stiffener shape (4)

Fig. 2 Finite element models used in the research

Fig. 3 Bilinear stress strain curve for steel   Fig. 4 Simplified compressive uniaxial stress strain curve for
                                                          concrete

linearly elastic up to its tensile strength of 3.5 N/mm^2 with elastic modulus equal to the initial modulus in compression.

3.3 Loads, boundary conditions and nonlinear analysis

A distributed pressure is applied at the surface of the column upper end plate. An initial imperfection of (1/1000) times the length of the column is considered. The end surfaces of the CFT column are free while ends of steel I-beams are restrained in which vertical stiffener plates are used. One end of the steel beam is modelled with all three translation degrees of freedom restrained U_x , U_y , U_z as well as the rotational degree of freedom about the beam longitudinal axis, R_z. The other end is modelled with two translation degrees of freedom restrained U_y and U_z except for the longitudinal direction of steel beam U_x, and also restraining the rotational degree of freedom, R_z. Fig. 5 shows schematic drawing of steel I-beam to CFT column connection with loading and support conditions. The "Newton-Raphson" approach is employed to solve geometric nonlinearity. The results are accurately estimated by incremental steps until failure occurs. Solution technique is the arc length method. No weld failure is studied, so common nodes for the steel beam and the steel column tube at the weld locations or for stiffener and steel I-beam flange are provided.

4. Verification of the proposed models

The results obtained from the finite element analysis are verified against the previous experimental results prepared by Lu (1997). These tests show the ultimate moment of the
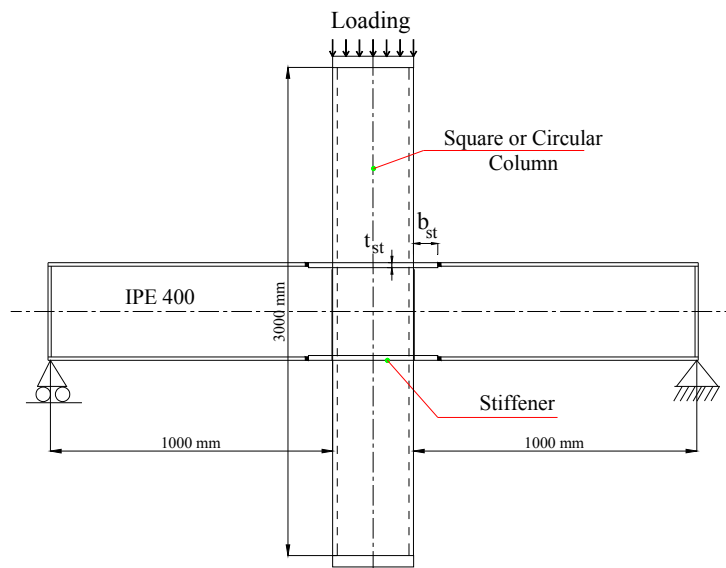

Fig. 5 Schematic drawing showing steel I-beam to CFT column connection with loading and support conditions adopted in the proposed finite element model

Table 1 Comparison between ultimate moment obtained by the proposed finite element model and those obtained by Lu (1997)

Specimen	M_{test} (kN.m)	M_{FEM} (kN.m)	M_{FEM}/M_{test}
3R1	48.5	50.5	1.04
3R2	32.4	30	0.92
3R3	44.5	43.8	0.98
		Mean	0.98
		Standard deviation	0.06

Table 2 Comparison between Ultimate Moment Obtained by the Proposed Finite Element Model and Those Obtained by Winkel (1998)

Specimen	M_{test} (kN.m)	M_{FEM} (kN.m)	M_{FEM}/M_{test}
3C1	82.5	90	1.09
3C2	54.1	51	0.94
3C3	79	87	1.10
		Mean	1.04
		Standard deviation	0.08

connection between steel I-beam, of IPE 240, and square CFT column, of 300×10, that is not filled with concrete under the effect of in-plane bending moment. The beam flange is welded to the column with butt weld, while the beam web is welded to the column on both sides of the web with fillet welds. The length of the column is 1800 mm, while the beam length is 1200 mm on each side. Column is loaded axially while beam ends are roller at one side and hinged at the other. The moment is obtained by multiplying the reaction force at beam support by the distance between the support and the column face.

Other experimental tests were conducted on connections between steel I-beams and circular CFT columns that are not filled with concrete under the effect of in-plane bending moment by Winkel (1998). Three specimens are tested with circular column of 324×9.5 and beam cross section of IPE 240, with the same lengths, connection method, loading cases and test setup used by Lu (1997). Tables 1 and 2 show the ultimate moment of the connection obtained from the tests, M_{test}, and that obtained from finite element analysis, M_{FEM}. The authors use the letter '*R*' to refer to square column and the letter '*C*' to refer to circular column followed by specimen number. The tables show that the results are in good correlation with the experimental results and validate the effectiveness of the adopted structural model.

5. Parametric study

An extensive parametric study using the finite element model described earlier is conducted. The effect of using stiffeners is illustrated by comparing each case involving presence of stiffener with another without a stiffener (unstiffened). Also, the effect of stiffener width (b_{st}) and stiffener thickness (t_{st}) is discussed. The studied b_{st} are 75, 100, 125 and 150 mm, while the studied t_{st} are

15 and 20 mm. The second parameter studied is the influence of changing the column cross section shape. Three columns cross sections are studied. The first is square column of 300×10 and the second is circular column of 500×15. The third column is also circular of 338×12 which is chosen to give an equivalent steel and concrete area to the first square column to compare the ultimate moment of the connection in both cases. The total column height is 3000 mm. The steel beam used is IPE 400 connected at the mid-height of the column with length 1000 mm on each side. All columns cross sections are chosen to cover the compactness limits according to ECP (2001), in which for square column width-to-thickness ratio is less than $[64/(F_y)^{0.5}]$ and for circular column diameter-to-thickness ratio is less than $[165/F_y]$, where F_y is the steel yield stress in (t/cm^2). Finally, the third parameter studied is the effect of filling the column cross section with concrete with compressive strength 35 N/mm^2. The results of the parametric study obtained are represented in the form of tables and curves. A ratio between ultimate moment of the connection and the plastic moment of the beam cross section (M_{ult}/M_p) is used in the figures. For more results of the parametric study, refer to Fawzy (2013).

6. Results and discussions

Tables 3-4 show the effect of stiffener configurations and dimensions on the ultimate moment of the connection between beam IPE 400 and square (300×10) and circular (500×15) columns respectively; while Table 5 demonstrates the effect of using an equivalent circular column (338×12). Finally, Tables 6-8 show the effect of filling the tubular columns with concrete.

6.1 Deformed shapes

When the columns are unstiffened, high distortion occurs in the steel column wall in which the failure occurs, as shown in Fig. 6. However, when the column is stiffened, two different failure

Table 3 Ultimate moment of the connection (kN.m) between IPE 400 and square column 300×10 not filled with concrete

Unstiffened column	Stiffening plate		Stiffener shape (1)	Stiffener shape (2)	Stiffener shape (3)	Stiffener shape (4)	Effect of Stiffener			
M_{ult1}	b_{st} (mm)	t_{st} (mm)	M_{ult2}	M_{ult3}	M_{ult4}	M_{ult5}	M_{ult2}/M_{ult1}	M_{ult3}/M_{ult1}	M_{ult4}/M_{ult1}	M_{ult5}/M_{ult1}
	75		250.3	281.5	287.2	158	3.0	3.3	3.4	1.9
	100	20	287.7	355.8	359.9	230.2	3.4	4.2	4.3	2.7
	125		289.2	412.9	419.7	263.6	3.4	4.9	5.0	3.1
83	150		335.5	445.8	445.8	292.2	4.0	5.3	5.3	3.5
	75		199	275.7	281.3	142.1	2.4	3.3	3.3	1.7
	100	15	262.9	301.6	322.4	186.4	3.3	3.63	3.8	2.2
	125		272.1	359.3	362.7	217.6	3.3	4.33	4.3	2.6
	150		305.9	385.8	403.1	284.7	3.6	4.6	4.8	3.4

Table 4 Ultimate moment of the connection (kN.m) between IPE 400 and circular column 500 × 15 not filled with concrete
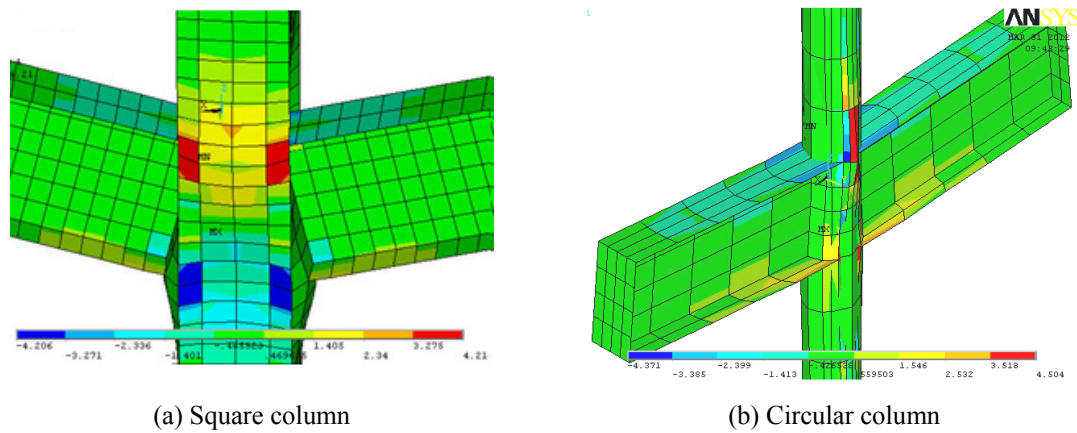
Unstiffened column	Stiffening plate		Stiffener shape (1)	Stiffener shape (2)	Stiffener shape (3)	Stiffener shape (4)	Effect of Stiffener			
M_{ult6}	b_{st} (mm)	t_{st} (mm)	M_{ult7}	M_{ult8}	M_{ult9}	M_{ult10}	M_{ult7}/M_{ult6}	M_{ult8}/M_{ult6}	M_{ult9}/M_{ult6}	M_{ult10}/M_{ult6}
	75		340.6	351.6	361.3	288.1	1.3	1.3	1.3	1.1
	100	20	342.7	363.7	375.6	329.06	1.3	1.4	1.4	1.2
	125		351.3	418.3	421.3	348.2	1.3	1.6	1.6	1.3
	150		415.7	445.7	445.7	356.4	1.6	1.7	1.7	1.3
259.3	75		263.3	266.4	275.1	261.2	1.02	1.03	1.06	1.01
	100	15	303.5	304.1	315.5	302	1.17	1.17	1.2	1.16
	125		315.2	356.9	356.5	319.6	1.2	1.38	1.38	1.2
	150		369.09	396.4	416.7	343.7	1.4	1.5	1.6	1.3

Table 5 Ultimate moment of the connection (kN.m) between IPE 400 and equivalent circular column 338 × 12 not filled with concrete

Unstiffened column	Stiffening plate		Stiffener shape (1)	Stiffener shape (2)	Stiffener shape (3)	Stiffener shape (4)
M_{ult6}	b_{st} (mm)	t_{st} (mm)				
	75		279	303.8	309.8	276.7
	100	20	320.7	360.6	363.7	318.8
	125		342.3	412.3	422.7	328.1
259.3	150		353.7	443.5	445.7	330.4
	75		275.3	280.3	302.1	272.2
	100	15	306.5	308	324.5	298.1
	125		326.8	362.4	365.6	302.6
	150		329	390	406	305.3

modes occur either at stiffener or at compression beam flange regardless of the column cross section shape because the maximum stresses are shifted away from the column. Failure occurs at the stiffener of dimensions 75 × 15 for square column with stiffener shape (1), as shown in Fig. 7(a), as well as for circular column with stiffener shape (4), as shown in Fig. 7(b). By increasing the stiffener dimensions and/or stiffening the column with stiffener shape (2), local buckling of the beam compression flange occurs for both square and circular columns, as shown in Figs. 7(c) and (d), respectively. Also, failure of the connection is observed locally at the beam compression flange for columns that are stiffened with stiffener shape (3), except for stiffeners 75 × 15 and 100 × 15, for both square and circular columns, as shown in Figs. 7(e) and (f), respectively. Failure of the connections occurs at stiffener shape (4) even with their big dimensions, width and thickness, which reduces the efficiency of the connection. Generally, failure of the connection at steel column wall and stiffeners shall be avoided and move towards beam flanges to obtain ductile

<table>
<tr><td>(a) Square column</td><td>(b) Circular column</td></tr>
</table>

(a) Square column   (b) Circular column

Fig. 6 Stress distribution (t/cm^2) of unstiffened column where failure occurs at the column steel wall

Table 6 Ultimate moment of the connection (kN.m) between IPE 400 and square column 300×10 filled with concrete

Unstiffened column	Stiffening plate		Stiffener shape (1)	Stiffener shape (2)	Stiffener shape (3)	Stiffener shape (4)
	b_{st} (mm)	t_{st} (mm)				
110.5	75	20	258.9	309.9	344.5	206.8
	100		322.8	360.6	374.9	320.1
	125		357.7	415.3	420.2	356.06
	150		385.7	445.7	445.7	366.04
	75	15	235	287.6	296.3	156.6
	100		283.2	305.9	329.6	281.02
	125		319.7	363.7	366.7	290.5
	150		340.6	393.5	409.2	323.9

Table 7 Ultimate moment of the connection (kN.m) between IPE 400 and circular column 500×15 filled with concrete

Unstiffened column	Stiffening plate		Stiffener shape (1)	Stiffener shape (2)	Stiffener shape (3)	Stiffener shape (4)
	b_{st} (mm)	t_{st} (mm)				
308	75	20	370.3	372.8	373.4	342.9
	100		374.9	386.7	397.1	351.5
	125		376.3	425.9	445.7	355.2
	150		426.97	445.7	445.7	365.7
	75	15	310.1	312.9	314.7	318.6
	100		315.2	317.5	320.5	325.5
	125		354.8	358.8	360.6	330.5
	150		377.8	399.3	420.6	349.4

Table 8 Ultimate moment of the connection (kN.m) between IPE 400 and equivalent circular column 338 ×
         12 filled with concrete

Unstiffened column	Stiffening plate		Stiffener shape (1)	Stiffener shape (2)	Stiffener shape (3)	Stiffener shape (4)
	b_{st} (mm)	t_{st} (mm)				
257.3	75	20	326.1	332.06	350.9	318.8
	100		360.6	379.2	385.7	339
	125		368.3	418.9	428.8	352.3
	150		389	445	445.7	369.09
	75	15	285.7	290.1	304.1	282.9
	100		314.5	322.9	326.5	305.02
	125		348	368.04	371.9	322.6
	150		350.2	398.4	408.5	329.3
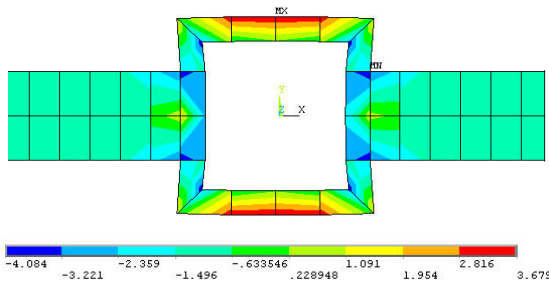
(a) Stress distribution (t/cm²) of column stiffened with stiffener shape (1) where failure occurs at the stiffener
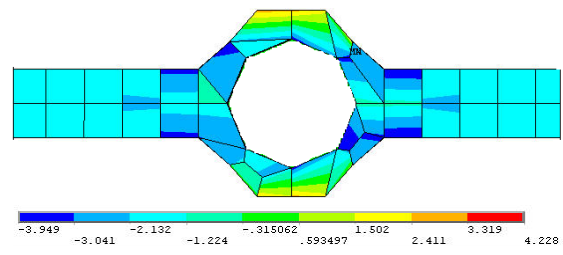
(b) Stress distribution (t/cm²) of column stiffened with stiffener shape (4) where failure occurs at the stiffener
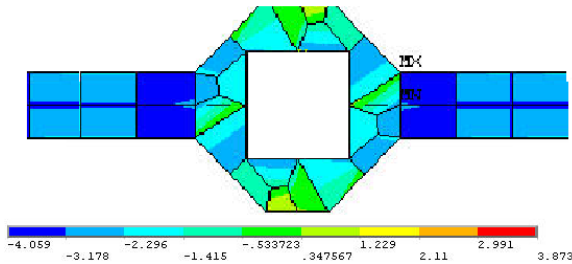
(c) Stress distribution (t/cm²) of square column stiffened with stiffener shape (2) where failure occurs at the beam compression flange
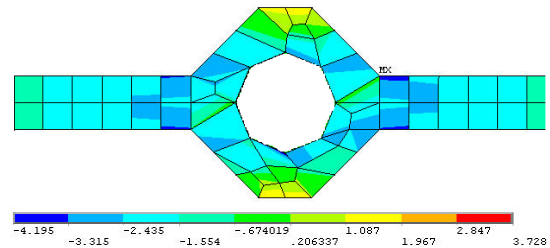
(d) Stress distribution (t/cm²) of circular column stiffened with stiffener shape (2) where failure occurs at the beam compression flange

Fig. 7 Different Stress distribution around the stiffened columns
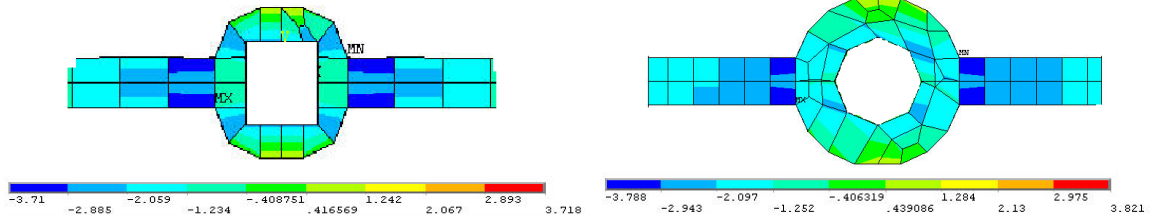
(e) Stress distribution (t/cm^2) of square column stiffened with stiffener shape (3) where failure occurs at the beam compression flange

(f) Stress distribution (t/cm^2) of circular column stiffened with stiffener shape (3) where failure occurs at the beam compression flange

Fig. 7 Continued
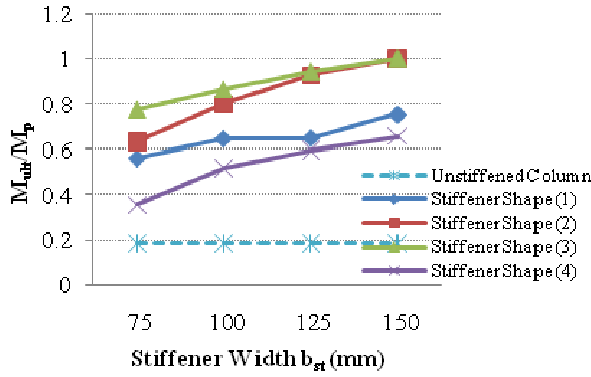
Fig. 8 M_{ult}/M_p ratio versus b_{st} of square column 300 × 10 due to different stiffener shapes, t_{st} = 20 mm
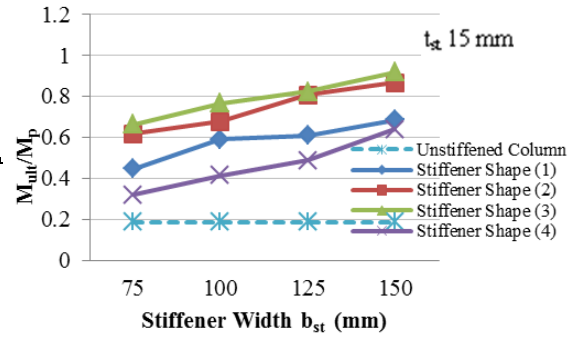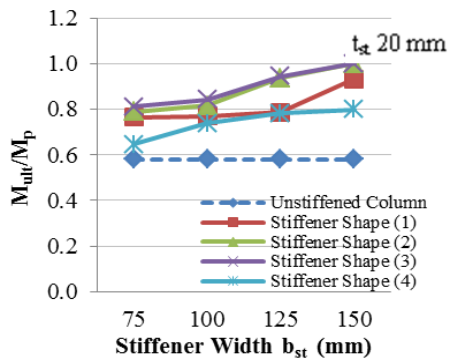
Fig. 9 M_{ult}/M_p ratio versus b_{st} of square column 300 × 10 due to different stiffener shapes, t_{st} = 15 mm

Fig. 10 M_{ult}/M_p ratio versus b_{st} of circular column 500 × 15 due to different stiffener shapes, t_{st} = 20 mm
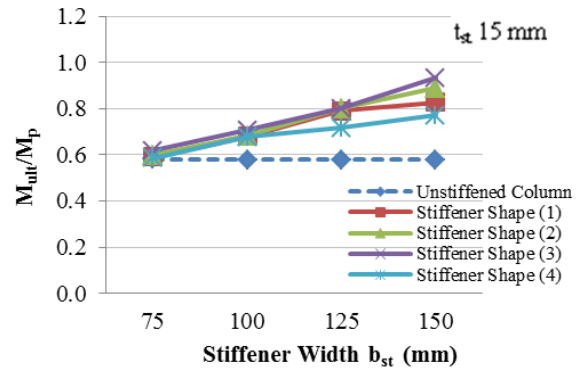
Fig. 11 M_{ult}/M_p ratio versus b_{st} of circular column 500 × 15 due to different stiffener shapes, t_{st} = 15 mm

connections. Concrete-filling of the columns does not change the location where failure occurs; it only reduces the deformation values.

6.2 Effect of stiffener configuration

Figs. 8 to 11 show the relation between (M_{ult}/M_p) ratio and different stiffener widths using the studied four stiffener shapes. It can be noticed that stiffener shape (3) gives the highest ultimate moment of the connections followed by stiffener shape (2), while stiffener shape (4) is the weakest. For square columns with stiffener shape (3) of 125×20, the increase is 45% compared to the connection with stiffener shape (1). Also, using stiffener 75×15, the values of ultimate moment of the connection using stiffener shape (3) are higher than that with stiffener shape (4) by about 98%. For circular column 500×15, the ultimate moment of the connection for column with stiffener shape (3), exceeds that stiffened with stiffener shape (1) of 125×20 by 19% and that stiffened with stiffener shape (4) of 75×15 by 25%.
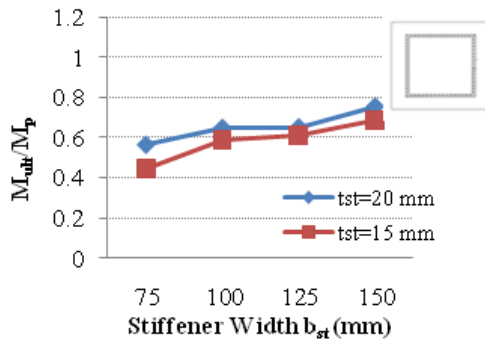
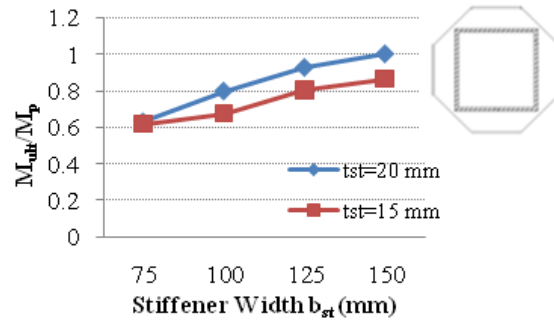Fig. 12 M_{ult}/M_p ratio versus b_{st} of stiffened column due to different t_{st}, stiffener shape (1)

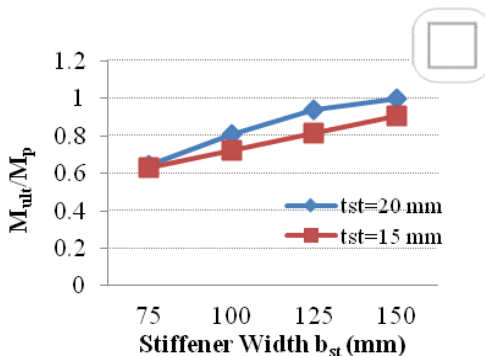Fig. 13 M_{ult}/M_p ratio versus b_{st} of stiffened column due to different t_{st}, stiffener shape (2)

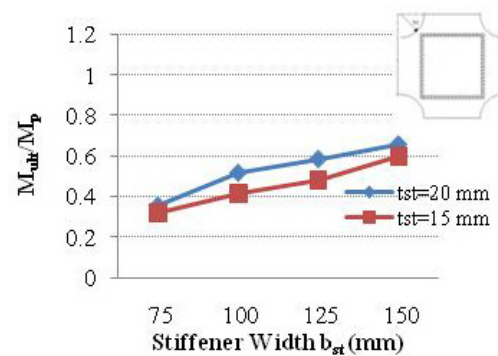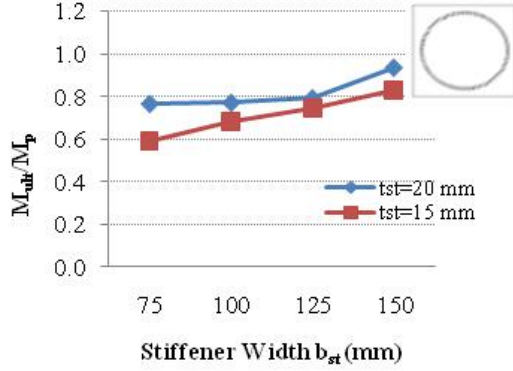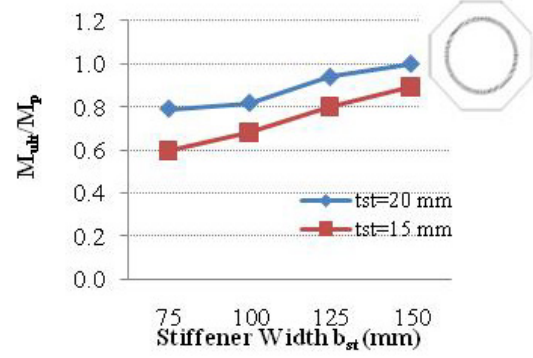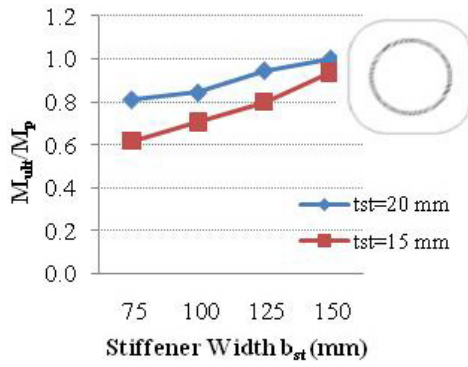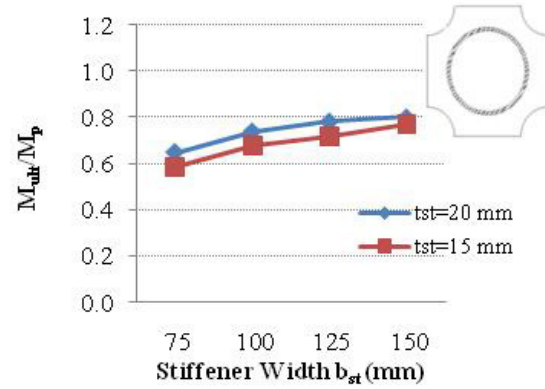Fig. 14 M_{ult}/M_p ratio versus b_{st} of stiffened column due to different t_{st}, stiffener shape (3)

Fig. 15 M_{ult}/M_p ratio versus b_{st} of stiffened column due to different t_{st}, stiffener shape (4)

Fig. 16 M_{ult}/M_p ratio versus b_{st} of stiffened column due to different t_{st}, stiffener shape (1)

Fig. 17 M_{ult}/M_p ratio versus b_{st} of stiffened column due to different t_{st}, stiffener shape (2)

Fig. 18 M_{ult}/M_p ratio versus b_{st} of stiffened column due to different t_{st}, stiffener shape (3)

Fig. 19 M_{ult}/M_p ratio versus b_{st} of stiffened column due to different t_{st}, stiffener shape (4)

6.3 Effect of stiffener dimensions

The increase in the ultimate moment of the connections is directly proportional to the stiffener dimensions, as shown in Tables 3 and 4. Using stiffener shape (1) with square column 300×10, the increase in the ultimate moment compared to the unstiffened column is about 2.40 times for smaller stiffener 75×15 and is up to 4.0 times for largest stiffener 150×20. Also, by comparing other stiffener shapes, the same conclusion can be noticed, as shown in Figs. 12 to 15. The maximum increase occurs with stiffener shape (2) and (3) of 150×20 which is about 5.30 times. However, using circular column 500×15, the increase in ultimate moment connection using different stiffener dimensions is small relative to square columns, as shown in Figs. 16 to 19. For example, using stiffener shape (1), the increase in the ultimate moment is about 1.02 times for smaller stiffener 75×15 and is up to 1.60 times for largest stiffener 150×20. The maximum increase occurs with stiffener shape (2) and (3) of 150×20 which is about 1.70 times.

6.4 Effect of column cross section shape

Table 5 shows the ultimate moment of the connection of circular column 338×12 which is chosen to give an equivalent steel and concrete area to the square column 300×10. By comparing results between circular and square columns, circular column is more efficient than the square column as it provides confinement that decreases local buckling of the column wall. Using stiffener shapes (1); the ultimate moment of the connection of circular column is greater than that of square column by 38% for stiffener 75×15 and only by 5% for stiffener 150×20, as shown in Figs. 20 and 21. However, they are almost the same for both circular and square columns with stiffener shapes (2) and (3), as shown in Figs. 22 to 25. Using stiffener shapes (4); the ultimate moment of the connection of circular column is greater than that of square column by 92% for stiffener 75×15 and only by 13% for stiffener 150×20, as shown in Figs. 26 and 27. This is because the maximum stresses are not shifted away from the column as sufficiently as the other shapes, so changing the column cross section shape is effective in this case.
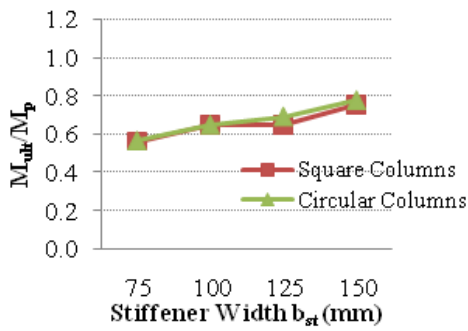

Fig. 20 M_{ult} / M_p ratio versus b_{st} of columns stiffened with stiffener shape (1), $t_{st} = 20$ mm
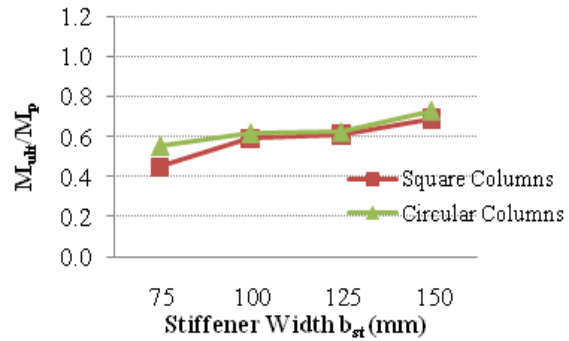
Fig. 21 M_{ult} / M_p ratio versus b_{st} of columns stiffened with stiffener shape (1), $t_{st} = 15$ mm
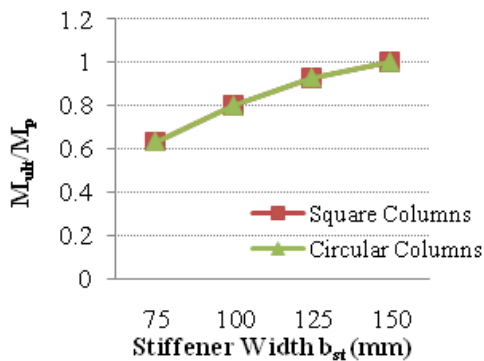

Fig. 22 M_{ult} / M_p ratio versus b_{st} of columns stiffened with stiffener shape (2), $t_{st} = 20$ mm

Fig. 23 M_{ult} / M_p ratio versus b_{st} of columns stiffened with stiffener shape (2), $t_{st} = 15$ mm

Fig. 24 M_{ult}/M_p ratio versus b_{st} of columns stiffened with stiffener shape (3), t_{st} = 20 mm

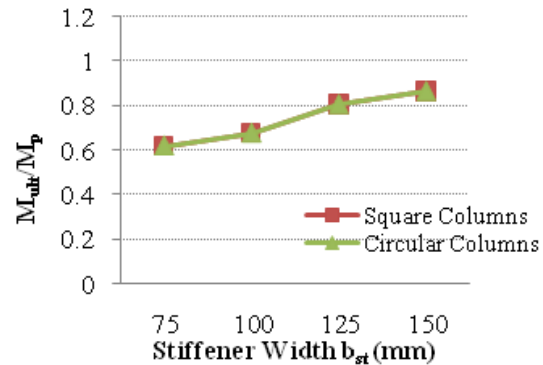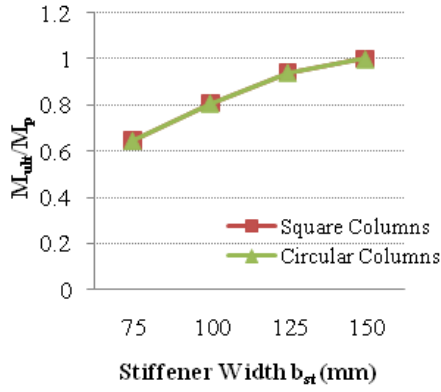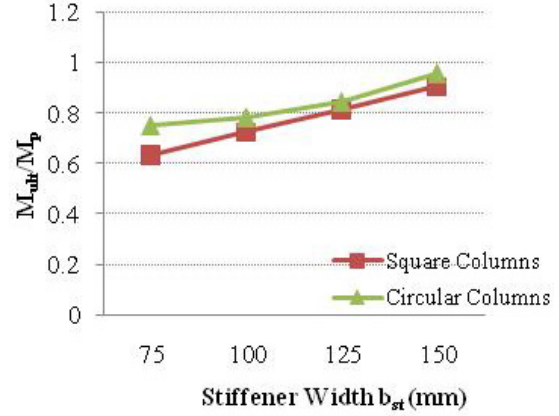Fig. 25 M_{ult}/M_p ratio versus b_{st} of columns stiffened with stiffener shape (3), t_{st} = 15 mm
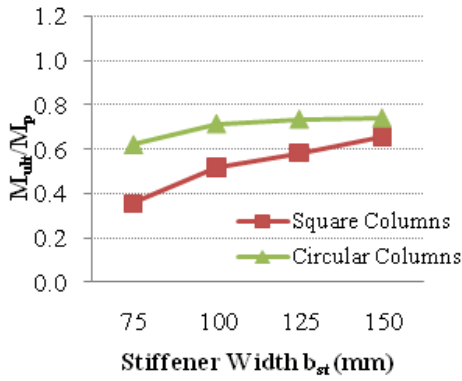

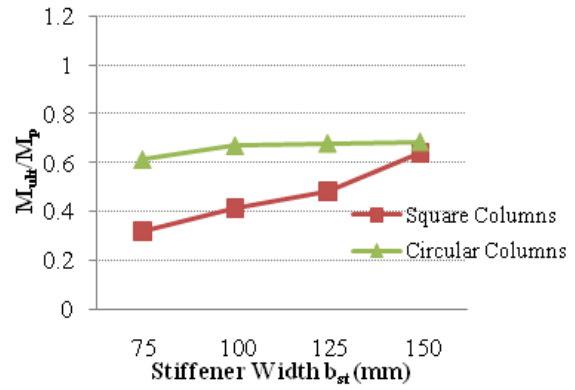Fig. 26 M_{ult}/M_p ratio versus b_{st} of columns stiffened with stiffener shape (4), t_{st} = 20 mm

Fig. 27 M_{ult}/M_p ratio versus b_{st} of columns stiffened with stiffener shape (4), t_{st} = 15 mm

6.5 Effect of filling the column cross section with concrete

For unstiffened columns, the ultimate moment of the connection is increased by up to 33% because it delays the local buckling of the column steel wall. For stiffened square column 300×10, the increase is up to 39% depending on stiffener shape and dimensions. For example, using stiffener shape (1), the increase in ultimate moment is about 18% for stiffener 75×15 and 15% for stiffener 150×20. Also, using stiffener shape (4), this increase is about 10% for stiffener 75×15 and 39% for stiffener 100×20. However, using stiffener shapes (2) and (3), the increase is less than 5% except for stiffener 75×15 where the increase is up to 20%. For stiffened circular column 500×15, the increase is up to 22% depending on stiffener shape and dimensions. For example, using stiffener shape (1), the increase in ultimate moment is about 18% for stiffener 75×15 and only 3% for stiffener 150×20. Also, using stiffener shape (4), the increase in ultimate moment is

about 22% for stiffener 75×15. The increase in the ultimate moment of the connection due to filling the column with concrete decreases as the stiffener dimensions increase especially for stiffener shapes (2) and (3) where the plastic moment of the beam is reached. Finally, the concrete fill of equivalent circular column 338×12 shows increase in ultimate moment of the connection by about 25% and 17% for unstiffened and stiffened columns, respectively.

7. Comparison between finite element analysis and Kurobane (2004)

Appendix A shows some of the simplified design equations using design guide Kurobane (2004). Table 9 demonstrates a comparison between the finite element results and those obtained using the simplified design equation (1) initially proposed by the design guide AIJ (1990) and modified by Kurobane *et al*. (2004). This data is for the moment connection between IPE 400 and the square column 300×10 with stiffener shape (4) not filled with concrete. The maximum difference in results is 11% which represents fair agreement. Also, Table 10 shows the same comparison where the square column is stiffened with stiffener shape (2) and filled with concrete with those of the design Eq. (2). A fair agreement between results is obtained and the maximum difference is 17%. Table 11 contains the comparison between the finite element results of circular

Table 9 Comparison between ultimate moment of the connection (kN.m) between IPE 400 and square column not filled with concrete and those obtained by Kurobane (2004)

Unstiffened column	Stiffening plate		Kurobane (2004) Eq. (1)	FEM (2014) by authors	Ratio FEM / Kurobane
	b_{st} (mm)	t_{st} (mm)			
300×10 with stiffener shape (4)	100	20	206.5	230.2	1.11
	125		240.5	263.6	1.09
	100	15	170.6	186.4	1.09
	125		198.7	217.6	1.09
				Mean	1.09
				Standard deviation	0.01

Table 10 Comparison between ultimate moment of the connection (kN.m) between IPE 400 and square column filled with concrete and those obtained by Kurobane (2004)

Unstiffened column	Stiffening plate		Kurobane (2004) Eq. (1)	FEM (2014) by authors	Ratio FEM / Kurobane
	b_{st} (mm)	t_{st} (mm)			
300×10 with stiffener shape (2)	100	20	352.14	415.3	1.17
	125		425.77	445.7	1.04
	100	15	307.2	363.7	1.18
	125		339.92	393.5	1.15
				Mean	1.14
				Standard deviation	0.06

Table 11 Comparison between ultimate moment of connection (kN.m) between IPE 400 and circular column stiffened filled with concrete and those obtained by Kurobane (2004)

Unstiffened column	Stiffening plate		Kurobane (2004) Eq. (1)	FEM (2014) by authors		Ratio FEM / Kurobane	
	b_{st} (mm)	t_{st} (mm)		Stiffener shape (2)	Stiffener shape (3)	Stiffener shape (2)	Stiffener shape (3)
500×15 with stiffener shapes (2) and (3)	75	20	300	372.8	373.4	1.24	1.24
	100		356.6	386.7	397.1	1.08	1.11
	125		416.03	425.9	445.7	1.02	1.07
	150		486.9	445.79	445.7	0.92	0.91
	75	15	241.8	312.9	314.7	1.29	1.30
	100		285.06	317.5	320.5	1.11	1.12
	125		328.4	358.8	360.6	1.09	1.09
	150		359.5	399.3	420.6	1.11	1.16
				Mean		1.10	1.12
				Standard Deviation		0.11	0.10

columns 500×15 with stiffener shapes (2) and (3) that are filled with concrete and those of the design Eq. (3). The results are in good correlation but it is worth to mention that Kurobane is conservative with stiffener width 75 mm.

8. Conclusions

The main conclusions obtained from this research can be summarized into the following:

- For unstiffened tubular columns, high distortion occurs in the steel column wall in which the failure occurs. However, two different failure modes occur for stiffened columns either at stiffener or at beam compression flange, regardless of the column cross section shape, because the maximum stresses are shifted away from the column.
- Presence of the stiffener at the outer column perimeter, which simplifies fabrication, reduces stress concentration, therefore the ultimate moment capacity of the connections of square and circular column cross sections is increased considerably.
- The most efficient stiffener which produces the highest ultimate moment of the connection is stiffener shape (3) which reduces the concentration of stresses at its curved corners, followed by stiffener shape (2) with its inclined sides, for both square and circular columns. Whereas, inevitable stress concentrations at the corners occur at the other stiffener shapes causing their premature failure.
- The increase in the ultimate moment of the connection is directly proportional to the stiffener dimensions. Increasing stiffener shape (1) from 75×15 to 150×20 increases the ultimate moment by up to 170% and 58% for square and circular columns, respectively.
- Circular column is advantageous than the square column for all stiffener shapes and dimensions as it provides confinement that decreases local buckling of the column wall.

- The ultimate moment of the connections of circular column cross section that is stiffened with stiffener shape (4) is higher than that of square column cross section by 92%. However, slight increase is observed when using stiffener shapes (2) and (3) as the maximum stresses are shifted away from the column.
- For unstiffened columns, the connections of circular column cross sections show higher ultimate moment than the square column cross section by up to 2.5 times.
- Filling the column cross section with concrete increases the ultimate moment of the connection by up to 33% and 39% for unstiffened and stiffened columns, respectively. The concrete-filling delays the local buckling of the steel column wall.
- The finite element analysis results are in fair correlation with those of the design guide equations of Kurobane (2004). However, Kurobane is conservative with stiffeners width 75 mm.

References

AIJ (1990), *Recommendations for the Design and Fabrication of Tubular Structures in Steel*, (3rd Edition), Architectural Institute of Japan, Tokyo, Japan.

ANSYS (2009), Finite Element Program, Swanson Analysis System Inc., Release 12.1.

Azizinamini, A. (2005), "Design of through beam connection detail for connecting steel beam to circular concrete-filled steel tube columns", *Steel Struct.*, **5**, 349-356.

Ellobody, E. and Young, B. (2006), "Nonlinear analysis of concrete-filled steel SHS and RHS columns", *Thin-Wall. Struct.*, **44**(8), 919-930.

Elremaily, A. and Azizinamini, A. (2001), "Experimental behavior of steel beam to CFT column connections", *J. Constructi. Steel Res.*, **57**(10), 1099-1119.

ECP No. (205) (2001), "Egyptian Code of Practice for Steel Construction and Bridges", Allowable Stress Design (ASD).

Fawzy, M.M. (2013), "Moment connections of beams and concrete-filled steel columns", Ph.D. Thesis, Faculty of Engineering, Ain Shams University, Egypt.

Fukumoto, T. (2005), "Steel beam to concrete-filled steel tube column, moment connections in Japan", *Steel Struct.*, **5**, 357-365.

Gere, J.M. and Timoshenko, S.P. (1997), "Mechanics of Materials", PWS Publishing Company, Boston, MA, USA.

Ju, Y.K., Kim, Y. and Kim, S. (2004), "FEM analysis on structural behavior of CFT column to flat plate slab connection", Report, University of Texas, Austin, TX, USA.

Kim, Y., Shin, K. and Kim, W. (2008), "Effect of stiffener details on behavior of CFT column-to-beam connections", *Steel Struct.*, **8**, 119-133.

Kimura, K., Chung, J., Matsui, C. and Choi, S. (2005), "Structural characteristics of H-shaped beam-to-square tube column connection with vertical stiffeners", *Int. J. Steel Struct., KSSC*, **5**(2), 109-117.

Kurobane, Y., Packer, J.A., Wardenier, J. and Yeomans, N. (2004), "Design guide for structural hollow section column connections", CIDECT, 9.

Lu, L.H. (1997), "The static strength of I-beam to rectangular hollow section column connections", Ph.D. Thesis, Faculty of Civil Engineering and Geosciences, Delft University of Technology, Netherlands.

Shin, K., Kim, Y., Oh, Y. and Moon, T. (2004), "Behavior of welded CFT column to H-beam connections with external stiffeners", *Eng. Struct.*, **26**(13), 1877-1887.

Wang, W., Han, L. and Uy, B. (2008), "Experimental behaviour of steel reduced beam section to concrete-filled circular hollow section column connections", *J. Construct. Steel Res.*, **64**(5), 493-504.

Wang, J., Han, L. and Uy, B. (2009), "Behaviour of flush end plate joints to concrete-filled steel tubular columns", *J. Construct. Steel Res.*, **65**(4), 925-939.

Wang, Y., Xuan, Y. and Mao, P. (2010), "Nonlinear finite element analysis of the steel-concrete composite beam to concrete-filled steel tubular column joints", *Int. J. Nonlinear Sci.*, **9** (3), 341-348.

Winkel, G.D. (1998), "The static strength of I-beam to circular hollow section column connections", Ph.D. Thesis, Faculty of Civil Engineering and Geosciences, Delft University of Technology, Netherlands.

Yao, H., Goldsworthy, H. and Gad, E. (2008), "Experimental and numerical investigation of the tensile behavior of blind-bolted T-stub connections to concrete-filled circular columns", *J. Struct. Eng.*, *ASCE*, **134**(2), 198-208.

CC

Appendix A: Simplified design equations using design guide Kurobane (2004)

The design of connections with stiffened CFT columns that are subjected to moment have been mainly initially studied in the Architectural Institute of Japan Recommendations AIJ (1990) and was modified by design guide CIDECT 9 Kurobane (2004). Both circular and square column cross sections are applicable. The following are some of the simplified design equations, mentioned in this design guide, for different stiffeners and columns shapes. For the range of validity of these equations, it can be referred to the design guide.

A.1 Ultimate load of square CFT column moment connection stiffened with stiffener shape (4) that is not filled with concrete, as shown in Fig. 28(a)

$$P_{b.f} = 3.17 \left[T / W_c \right]^{2/3} \left[t_{st} / W_c \right]^{2/3} \left[(T_c + h_d) / W_c \right]^{1/3} \left[W_c \right]^2 F_{yst} \qquad (1)$$

A.2 Ultimate load of square CFT column moment connection stiffened with stiffener shape (2) that is filled with concrete, as shown in Fig. 28(b)

$$P_{b.f} = 2.86 \left[4T_c / t_{st} \right] T_c F_{yc} + 3.30 h_d t_{st} F_{yst} \qquad (2)$$

A.3 Ultimate load of circular CFT column moment connection stiffened with stiffener shapes (2) and (3) that is filled with concrete, as shown in Fig. 28-c

$$P_{b.f} = 3.09 A_1 F_{yc} \sin\alpha + 1.77 A_2 F_{yst} \left[2\sin^2\alpha + 1 \right]^{0.5} \qquad (3)$$

Where
$P_{b.f}$ =   Ultimate load in tension or compression flange (ton)
F_{yc} =   Yield stress of column (t/cm^2)
F_{yst} =   Yield stress of stiffener (t/cm^2)
W_c =   Column width (cm)
D_c =   Column diameter (cm)
T_c =   Column wall thickness (cm)
t_{st} =   Stiffener thickness (cm)
t_f =   Compression beam flange thickness (cm)
h_d =   Stiffener dimension (cm)
θ =   Slope of critical section
A_1 = $[(0.63 + 0.88 b_f / D_c) (D_c T_c)^{0.5} + t_{st}] T_c$
A_2 = $b_{st} t_{st}$
b_f =   Compression beam flange width (cm)
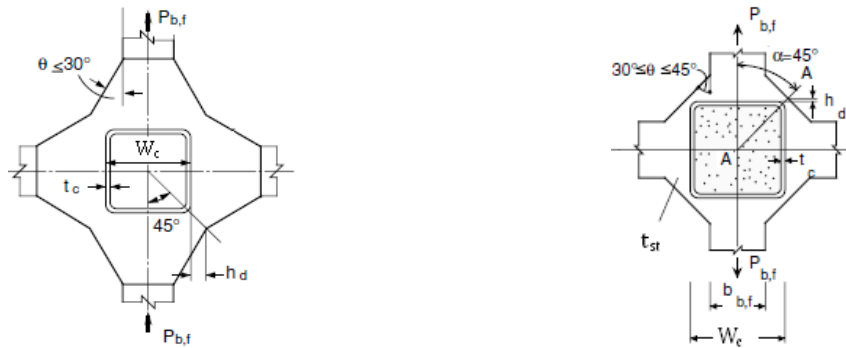
(a) Square column with stiffener shape (4) not filled with concrete

(b) Square column with stiffener shape (2) filled with concrete
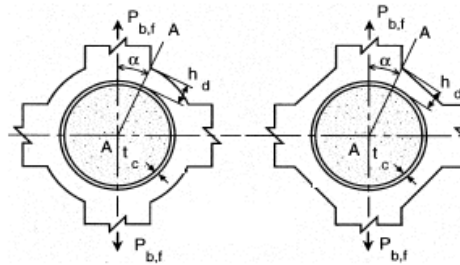
(c) Circular column with stiffener shapes (2) and (3) filled with concrete

Fig. 28 Different symbols used in design equations for connection of square and circular columns with different stiffener shapes according to Kurobane (2004)